Fermi National Accelerator Laboratory

FN-484

Beam-Gas Scattering Lifetimes in the Fermilab Main Ring

M. J. Syphers
Fermi National Accelerator Laboratory
P.O. Box 500, Batavia, Illinois 60510

May 5, 1988

Operated by Universities Research Association Inc. under contract with the United States Department of Energy

Beam-Gas Scattering Lifetimes in the Fermilab Main Ring

M. J. Syphers

May 5, 1988

Since its commissioning, the Fermilab Main Ring synchrotron has experienced short beam lifetimes at the injection (total) energy of 8.9 GeV. Because of the repetitive injection cycles from the Booster synchrotron, many particles must coast at the injection energy for nearly one second during most Main Ring operations. With a lifetime at 8.9 GeV of a few seconds at best, a significant fraction of the beam intensity is lost during the injection process. This loss, coupled with other beam losses which occur at the beginning of acceleration as well as at the crossing of the transition energy (17.5 GeV), has led to the examination of other injection energies for this device.

Recent accelerator experiments, during which beams were allowed to coast at constant energy for many seconds, have indicated that the 8.9 GeV lifetime in the Main Ring lies typically in the range of 1 - 30 secs. while the lifetime at 20 GeV is many hundreds of seconds. It was known that the field quality of the main bending magnets is worse at 8.9 GeV than at 20 GeV due to the strong remanent fields present at low excitation. This, coupled with the smaller beam size at 20 GeV, leads one to suspect that the lifetime should be improved at 20 GeV and, in fact, may be accounted for by beam-gas scattering.

This document provides estimates of what lifetimes should be expected due to beam-gas multiple scattering on the time scales accessible to the Main Ring at various energies and compares these numbers with the observations made during the studies mentioned above. The model used has been employed previously by Teng, [1] Snowdon, [2] and others to study Main Ring beam performance, though during those earlier studies the 8.9 GeV lifetime was no larger than 0.5 secs. Differences between beams that initially fill the aperture and beams that do not were not discussed.

---

[1]Teng, L. C., "Pressure Dependence of the decay of the Main Ring Coasting Beam," EXP-1, Fermilab Internal Report, 1972.

[2]Snowdon, S. C., "Residual Gas Analysis in Main Ring to Obtain Mean-Square Scattering Angle and Beam Lifetime," TM-341, Fermilab Internal Report, 1972.

Reduction of the Problem

The initial distribution of particles in transverse phase space is denoted by $f_o(x, x')$, where x is the transverse coordinate and x' is the slope of a particle's trajectory, $x' = dx/ds$. In the absence of scattering, we assume that this distribution will not change with time, and so

$$f(x, x', t) = f_o(x, x').$$

However, when elastic scattering takes place between the gas particles and the beam particles, the extent of the distribution will grow with time and $f(x, x', t)$ will satisfy the diffusion equation.

The problem is best approached by transforming the coordinates to involve the Courant-Snyder invariant $W = \frac{1}{\beta}(x^2 + (\alpha x + \beta x')^2) \equiv r^2/\beta$. Thus, we may write $f = f(W, t)$ since the variable W is independent of longitudinal location within the accelerator. The diffusion equation then becomes

$$\frac{\partial f}{\partial t} = D \frac{\partial}{\partial W}\left(W \frac{\partial f}{\partial W}\right)$$

where $D =< dW/dt >$ is the average rate of change of W with respect to time. To proceed, we define two quantities:

$$\begin{aligned} Z &= \frac{W}{W_a} \\ \tau &= \left(\frac{D}{W_a}\right) t \end{aligned}$$

where W_a is the Courant-Snyder invariant corresponding to the aperture of the machine (i. e., the admittance). If a is the half-aperture at a particular location where the amplitude function has the value β, then $W_a = a^2/\beta$. Notice that Z and τ are both dimensionless quantities.

In terms of Z and τ, the problem reduces to

$$\frac{\partial f}{\partial \tau} = \frac{\partial}{\partial Z}\left(Z \frac{\partial f}{\partial Z}\right) \tag{1}$$

subject to the boundary conditions

$$f(Z, 0) = f_o(Z)$$

$$f(1, \tau) = 0.$$

The solution of the above differential equation is

$$f(Z, \tau) = \sum_n c_n J_o(\lambda_n \sqrt{Z}) e^{-\lambda_n^2 \tau/4} \tag{2}$$

with

$$c_n = \frac{1}{J_1(\lambda_n)^2} \int_0^1 f_o(Z) J_o(\lambda_n \sqrt{Z}) dZ \tag{3}$$

where λ_n is the nth zero of the Bessel function $J_o(z)$.

We now consider a particular form of the initial distribution, namely a bi-gaussian in $x - x'$ phase space. For this situation, the function f_o will be

$$\begin{aligned} f_o(x,x')dxdx' &= \frac{1}{2\pi\sigma^2}e^{-(x^2+(\alpha x+\beta x')^2)/2\sigma^2}\beta dxdx' \\ &= \frac{1}{2\pi\sigma^2}e^{-r^2/2\sigma^2}rdrd\theta \\ &= \frac{1}{2}e^{-r^2/2\sigma^2}d(r^2/\sigma^2) \end{aligned}$$

or,

$$f_o(Z)dZ = \frac{a^2}{2\sigma^2}e^{-(a^2/2\sigma^2)Z}dZ.$$

So, the coefficients c_n become

$$c_n = \frac{\alpha}{J_1(\lambda_n)^2}\int_0^1 e^{-\alpha Z}J_o(\lambda_n\sqrt{Z})dZ,$$

where $\alpha = a^2/2\sigma^2$. If the entire initial beam distribution lies well within the aperture so that the integrand is sufficiently near zero before Z approaches 1, i.e., if α is greater than about 5, then the c_n's may be approximated by

$$\begin{aligned} c_n &= \frac{1}{J_1(\lambda_n)^2}e^{-x_n}(\cosh x_n - \sinh x_n) \\ &= \frac{1}{J_1(\lambda_n)^2}e^{-2x_n} \end{aligned}$$

where

$$x_n = \frac{\lambda_n^2}{4}\left(\frac{\sigma}{a}\right)^2.$$

If the initial distribution does not satisfy the above condition, then the c_n integrals must be performed numerically.

The development of the particle distribution with time, as well as the total beam intensity as a function of time, may now be estimated. By integrating $f(Z,\tau)$ over the range of Z, the number of particles $N(\tau)$ may be obtained, namely,

$$\begin{aligned} N(\tau) &= \int_0^1 f(Z,\tau)dZ \\ &= \int_0^1 \sum_n c_n J_o(\lambda_n\sqrt{Z})e^{-\lambda_n^2\tau/4}dZ \end{aligned}$$

or,

$$N(\tau) = 2\sum_n \frac{c_n}{\lambda_n}J_1(\lambda_n)e^{-\lambda_n^2\tau/4}. \tag{4}$$

For $\sigma \ll a$, this becomes

$$N(\tau) = 2\sum_n \frac{1}{\lambda_n J_1(\lambda_n)} e^{-\frac{\lambda_n^2}{4}\left[\tau + 2\left(\frac{\sigma}{a}\right)^2\right]}.$$

By plotting $N(\tau)$ vs. τ and $f(Z,\tau)$ vs. $\sqrt{Z}$ for various τ, lifetimes and emittance growths may be obtained. Figure 1 shows how $f(Z,\tau)$ varies with time for the case $\sigma/a = 0.20$. The particle distribution grows in transverse size until it reaches the aperture (Z=1) at which time the area under the curve quickly begins to decrease. The intensity $N(\tau)$ for this same case is displayed in Figure 2. From $\tau = 0$ to $\tau \approx 0.1$ the intensity is relatively constant. Upon reaching the aperture limit, the intensity rapidly falls off until $\tau \approx 0.5$, where the final lifetime $4/\lambda_1^2$ is reached. When a substantial fraction of the initial Gaussian distribution lies outside the aperture limit (all particles with $Z > 1$ being lost immediately) the rather flat region of $N(Z)$ for small Z disappears. Figure 3 shows the intensity vs. time for the case $\sigma/a = 0.4$. The lifetime, determined by

$$\tau_L(\tau) = -\frac{N(\tau)}{dN/d\tau} \tag{5}$$

is shown in Figure 4 for the two cases $\sigma/a = 0.2, 0.4$. The one case begins with a very long lifetime which then decreases to the value $4/\lambda_1^2$, while the other case begins with a very short lifetime and rapidly approaches its asymptotic value.

Evaluation of Diffusion Constant for Main Ring Environment

The dimensionless quantity τ is related to time t by

$$\tau = \left(\frac{D}{W_a}\right) t.$$

Now, $D = < dW/dt >$ and $dW = d[(x^2 + (\alpha x + \beta x')^2)/\beta] = (2\alpha x dx' + \beta^2 dx'^2)/\beta$ due to scattering. Thus,

$$\begin{aligned} D &= < \beta \frac{d}{dt}(dx'^2) > \\ &= \bar{\beta}\dot{\theta}^2_{rms}, \end{aligned}$$

where $\dot{\theta}^2_{rms}$ is the projected angle appropriate to a radiation length, given by

$$\begin{aligned} \dot{\theta}^2_{rms} &= \left(\frac{.015GeV}{vp}\right)^2 \frac{c}{L_{rad}} \\ &= \left(\frac{.015GeV}{mc^2\gamma}\right)^2 \frac{c}{L_{rad}} \\ &= (3.3 \times 10^{-7}/sec)\frac{P[\mu torr]}{\gamma^2} \end{aligned}$$

assuming air for the residual gas in the vacuum chamber, and assuming $v \approx c$. Here, γ is the Lorentz factor, $\bar{\beta}$ is the average value of the amplitude function around the machine, and $P[\mu torr]$ is the average vacuum chamber pressure expressed in microtorrs. The ratio t/τ may thus be written as

$$\begin{aligned} t/\tau &= \frac{W_a}{D} = \left(\frac{a^2}{\beta}\right)/D \\ &= \left(\frac{\bar{a}^2}{\bar{\beta}}\right)\frac{1}{\bar{\beta}\dot{\theta}^2_{rms}} \end{aligned}$$

or,

$$t/\tau = (3 \times 10^6 sec)\left(\frac{\bar{a}}{\bar{\beta}}\right)^2 \frac{\gamma^2}{P[\mu torr]}. \tag{6}$$

The quantity $\bar{a}$ is the effective half-aperture at a location of average amplitude function $\bar{\beta}$. For the Main Ring, the average value of the amplitude function is approximately 50 m.

At Fermilab, beam emittances and admittances are typically quoted as areas in phase space in which 95% of the presumed Gaussian distribution of particles is contained, normalized to the beam energy. To turn these phase space areas into beam sigmas and apertures, we use

$$\begin{aligned} emittance = \epsilon_N &\equiv \frac{6\pi\sigma^2}{\beta}(\gamma) \\ admittance = \hat{\epsilon_N} &\equiv \frac{\pi a^2}{\beta}(\gamma) \end{aligned}$$

Using these definitions, the ratios t/τ and σ/a may be written as

$$t/\tau = (3 \times 10^6 sec)\frac{\gamma\hat{\epsilon_N}/\pi}{\bar{\beta}P[\mu torr]} \tag{7}$$

$$\sigma/a = \sqrt{\frac{\epsilon_N}{6\hat{\epsilon_N}}}. \tag{8}$$

Comparisons with Measurements

A series of measurements taken during the last several months at 8.9 GeV and 20 GeV total energies in the Main Ring have revealed the following beam characteristics:

- The vertical admittance at 8.9 GeV is roughly 15 π mm mr. The horizontal admittance is over 30 π mm mr.
- Low intensity beams at 8.9 GeV start with a shorter lifetime and quickly develop a constant lifetime of about 30 sec., experience slow emittance growth, and have initial emittances of about 12 π mm mr.

- High intensity beams at 8.9 GeV have a variable lifetime from a fraction of a second immediately upon injection to roughly 30 sec. after coasting for many seconds. These beams have initial emittances of about 15 π mm mr which tend to decrease during coasting.

- The vertical admittance at 20 GeV is roughly 44 π mm mr while the horizontal admittance was never directly measureable and is assumed large ($> 75\pi$ mm mr).

- Beams at all intensities at 20 GeV experience slow emittance growth during coasting at that energy. The beam lifetime is greater than 600 sec. (limited by the detector resolution) during the first 5 sec. of coasting.

The above observations were made by measuring beam intensity and transverse beam profiles during a five second "coasting" period at the energy of interest. During these studies the average pressure in the Main Ring as measured by the vacuum gauges located periodically throughout the tunnel was $P \approx 3 \times 10^{-7}$ torr. (Since this vacuum pressure is obtained by monitoring the current drawn by the vacuum pumps, this estimate may be optimistic.) However, use of this number, coupled with the admittances and emittances quoted above, yields

Energy	t/τ	σ/a
8.9 GeV	36 sec.	0.4
20 GeV	180 sec.	0.2

Since the vertical admittance is much smaller than the horizontal admittance, the only case studied here, which is reflected by the numbers in the above table, is the vertical plane. The 8.9 GeV numbers quoted are for the low intensity beam case.

Figure 5 is a plot of $N(t)$ vs. t at 8.9 GeV using the above scaling. The lifetime at $t = 5$ sec. in this case, as shown in Figure 6, is roughly 30 sec. Figure 7 is data taken on January 14, 1988 and indicates a lifetime of 32 sec., 4.5 sec. after injection. The expected emittance growth due to gas scattering is shown in Figure 8 along with the measured emittance growth. At higher intensities, and correspondingly higher initial emittances, the emittance actually decreases with time at 8.9 GeV and the observed lifetime is assumed to be caused by a different mechanism.

Until January 15, 1988, only 5 sec. coasts were studied at 20 GeV during which no apparent beamloss was observable, yielding a lower bound for the lifetime of 600 sec. On this date a 10 sec. store was initiated for the first time and, after about 8 sec., the lifetime was seen to decrease gradually. Figures 9 — 11 show the predicted behavior at 20 GeV and that observed. Since the beam is injected, accelerated, and passed through transition before reaching 20 GeV, the rate at which the emittance grows once at 20 GeV was difficult to compare with the beam-gas model. During the 10 sec. store, however, the emittances did indeed grow by approximately 10 percent. The expected growth of an injected 20 GeV gaussian beam during a 10 sec. coasting period would be about 50 percent.

By inducing betatron oscillations, say through the use of a pulsed kicker magnet, the emittance may be increased and the behavior of larger emittance beams simulated. If a

gaussian distribution is displaced by an amount Δx the resulting distribution in phase space will become

$$f_o(Z) = \frac{a^2}{2\sigma^2}\left[I_o\left(\frac{\Delta x a}{\sigma^2}\sqrt{Z}\right)e^{\left(\frac{\Delta x a}{\sigma^2}\sqrt{Z}\right)}\right]e^{-(a\sqrt{Z}-\Delta x)^2/2\sigma^2}.$$

Using this distribution function, the corresponding c_n's in the expression for $N(\tau)$ may be computed numerically, or, for $\sigma \ll a$, we have

$$c_n = \frac{1}{J_1(\lambda_n)^2}J_o\left(\frac{\lambda_n \Delta x}{a}\right)e^{-\frac{\lambda_n^2}{4}\frac{2\sigma^2}{a^2}}.$$

Figure 12 shows the function $f_o(Z)$ for $\sigma/a = 0.2$ and for $\Delta x/\sigma = 2$. The intensity as a function of time for various kick amplitudes is shown in Figure 13 and the corresponding plots of lifetime as functions of time are shown in Figure 14. Figure 15 compares the lifetime resulting from the injection of a large emittance beam into a machine with the lifetime resulting from an initially small emittance beam which has been kicked.

During a series of 20 GeV measurements taken to determine the admittance of the ring (November 23, 1987), emittances and lifetimes were recorded 2.75 sec. after the beam had been kicked. Figure 16 displays the measured lifetimes along with those expected from the calculations described above. Values of $\sigma/a = .28$ and $t/\tau = 100$ sec. were used which are within the typical range of operating conditions, although they were not measured on this particular date. The main point to be made is that lifetimes much smaller than the "infinite" 600 sec. should be expected when large betatron oscillations are induced.

On February 8, 1988 a measurement was made during which beam was allowed to coast at 20 GeV for nearly two minutes. Here, the initial emittances were roughly 14 π mm mr in each plane. The beam intensity decreased with time in a fashion consistent with the beam-gas scattering model. (See Figure 17.) However, the rate of increase of emittance was a factor of two slower than predicted by the model. The machine was not as well tuned prior to this measurement as it had been for previous studies. A later study showed that by adjusting the tunes of the machine, the lifetime could be made "infinite" (>600 sec.) over the first 10 sec. at 20 GeV. Since then, a two minute store at 20 GeV has not been attempted. A repeat of this experiment and many of the others described above are scheduled for later this Spring.

Concluding Remarks

The general beam behavior at 20 GeV is consistent with beam-gas scattering, with lifetimes on the order of many hundreds of seconds observed over many seconds. Thus, one would anticipate that the efficiency of the Main Ring would be greatly increased by raising the injection energy to 20 GeV. During the admittance studies of November 23, 1988, long ($\sim$ 70 sec.) lifetimes were observed for beams with emittances of 20 π mm mr. (These emittances are expected for 20 GeV injection of high intensity beams after the proposed upgrade.)

The lifetimes observed at 8.9 GeV with low intensity, low emittance beams are also consistent with the beam-gas model. However, the initial losses observed with high intensity beams are indicative of other processes. From magnet measurements it is known that the multipole components of the Main Ring magnets are much larger at 8.9 GeV than at 20 GeV due to the remanent fields present at lower excitations. Tracking studies are underway to deterimine if one can explain the initial short lifetimes seen at 8.9 GeV with high intensity, high emittance beams using the magnet measurement results.

Further studies will take place during the upcoming Collider start-up. Repeats of the two minute stores at 8.9 GeV and 20 GeV are planned as well as further investigations of the behavior of large emittance beams at 20 GeV.

The author would like to express thanks to Rod Gerig, Steve Holmes, and Don Edwards for their contributions to the measurements and analysis of the wealth of data taken during the 8.9 GeV and 20 GeV studies, and for their help in preparing this document.

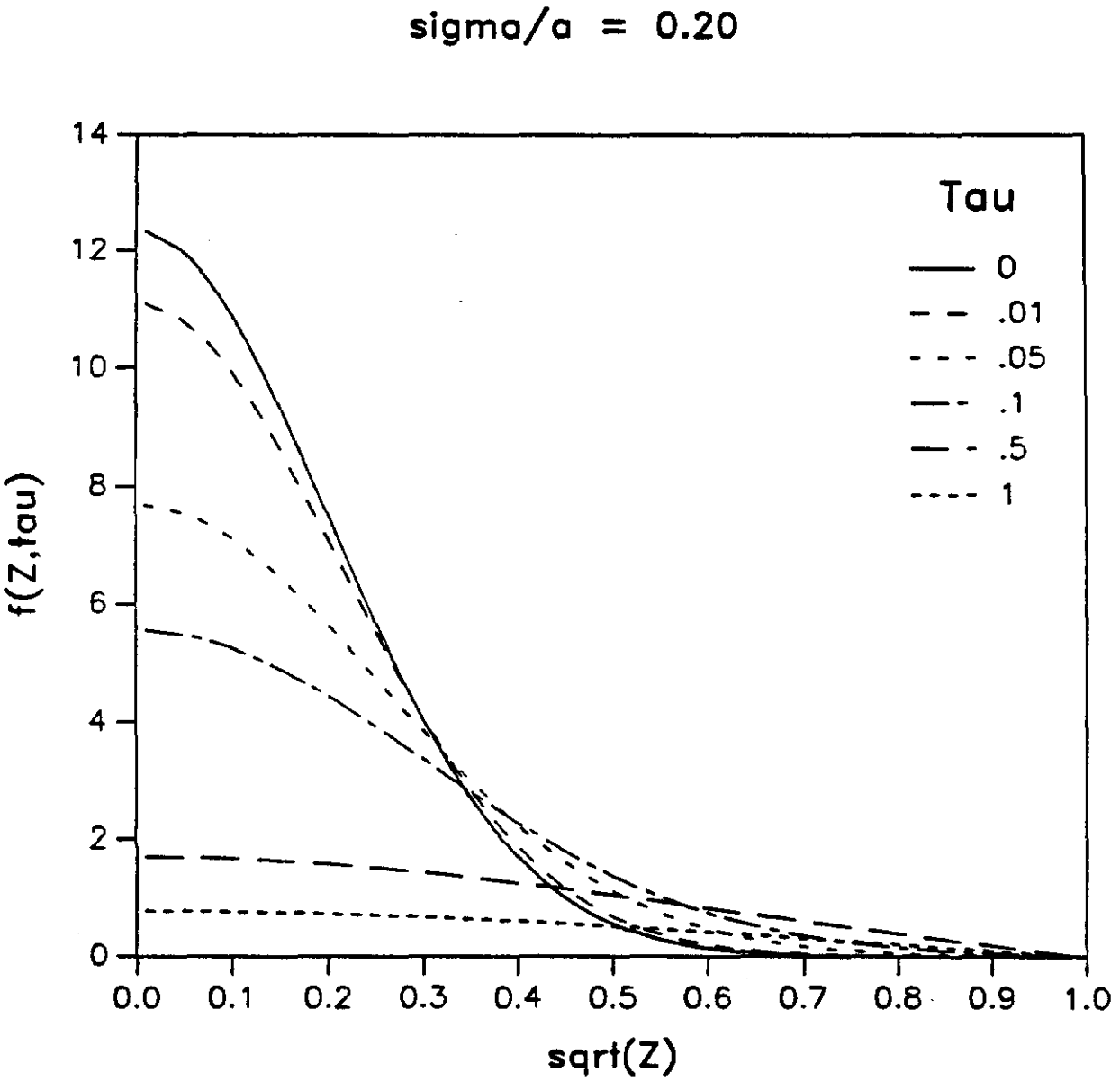

Figure 1. Development of particle distribution with time for beam-gas scattering model.

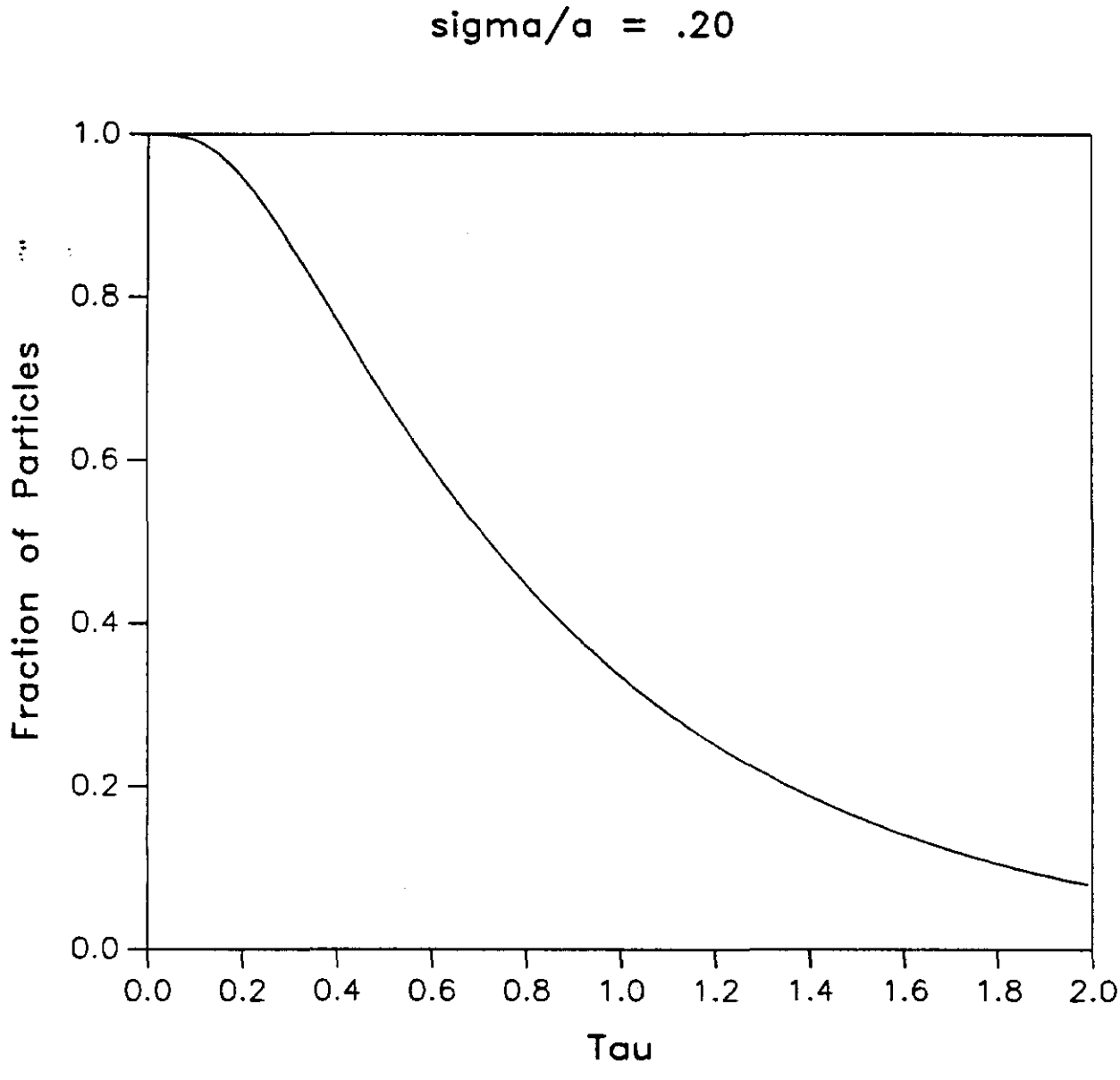

Figure 2. Beam intensity vs. "time" for a beam which is initially well contained within the machine aperture.

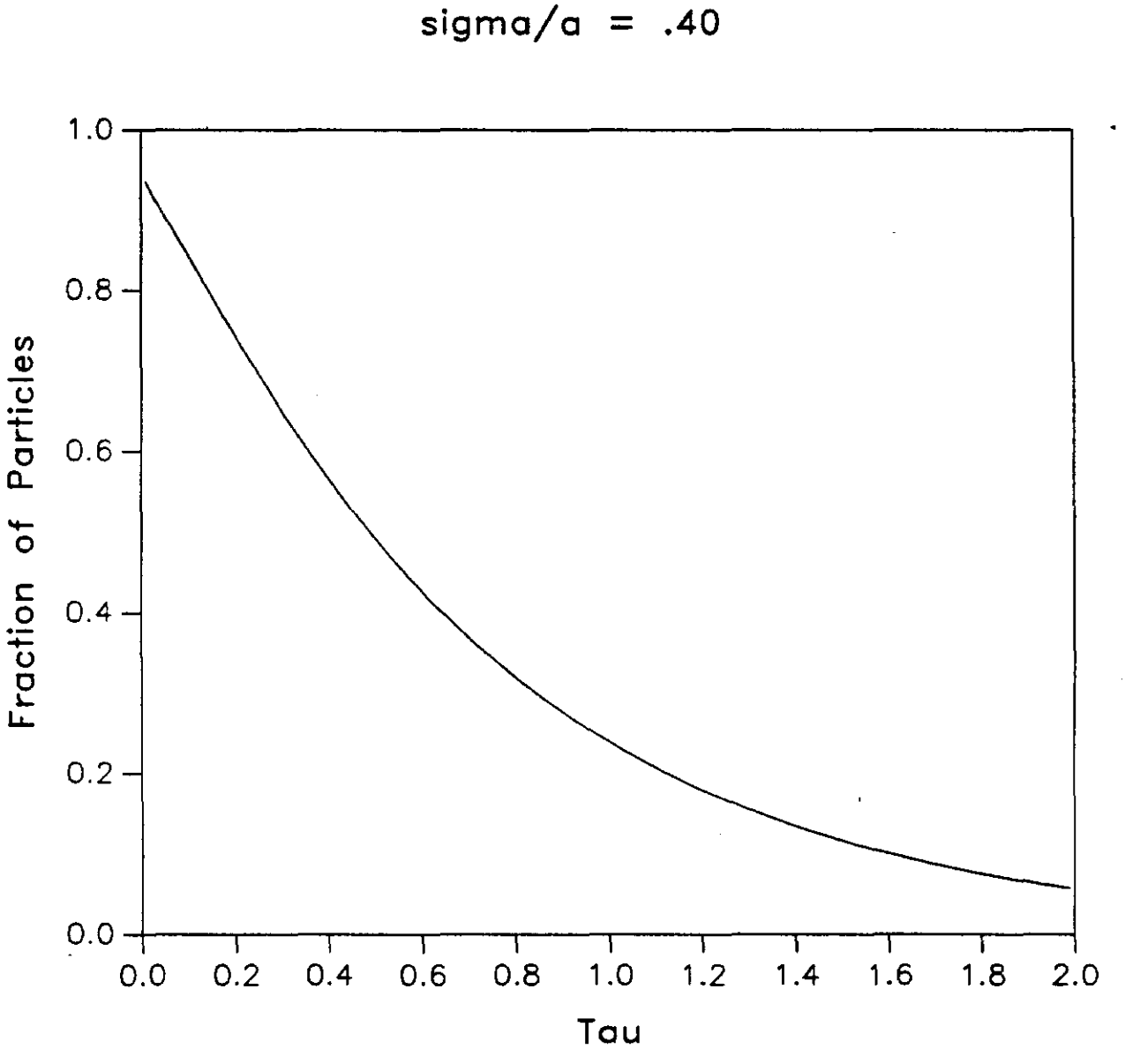

Figure 3. Beam intensity vs. "time" for a beam which extends to the machine aperture.

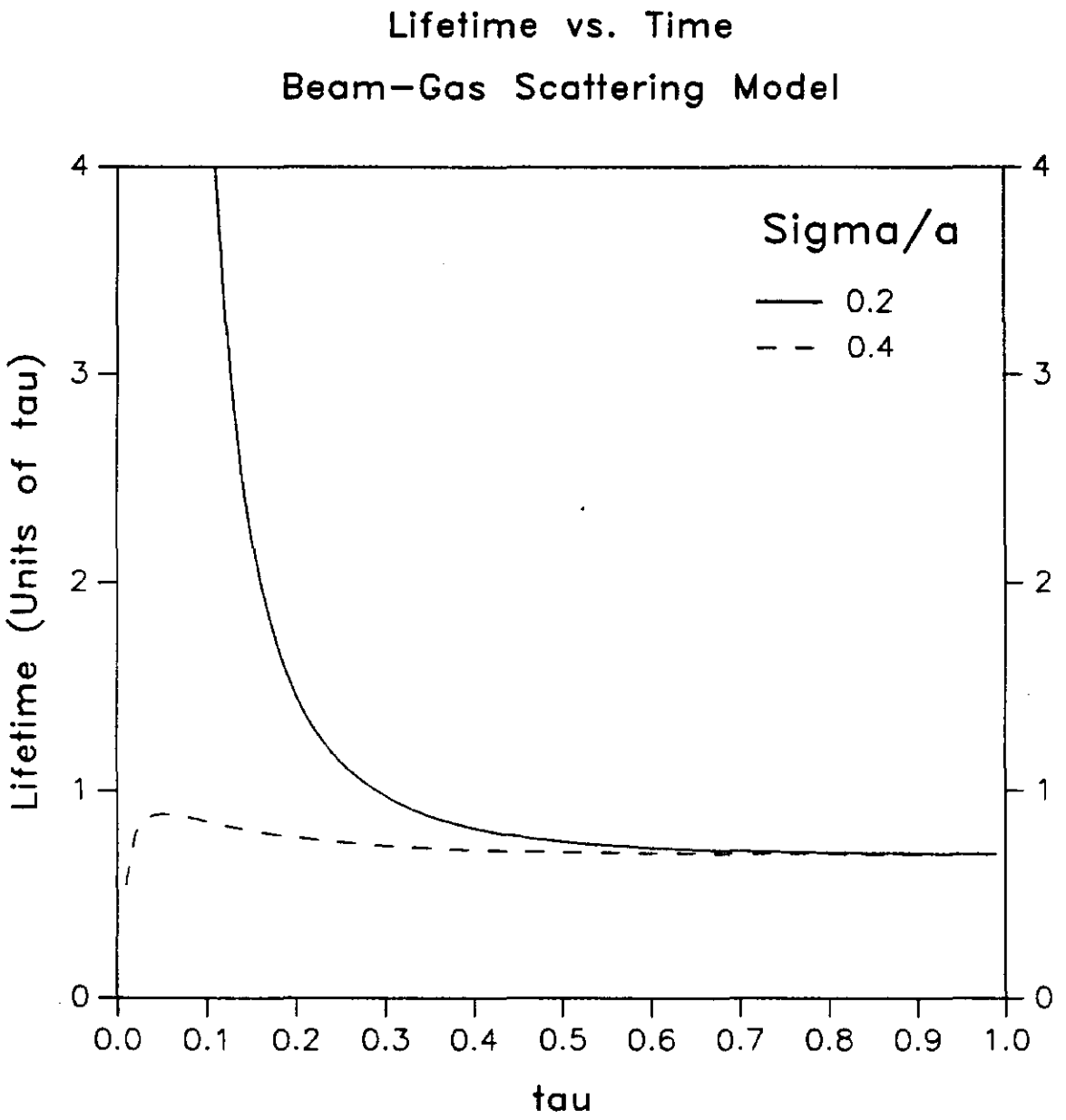

Figure 4. Beam lifetime vs. "time" for the cases described in the two previous figures.

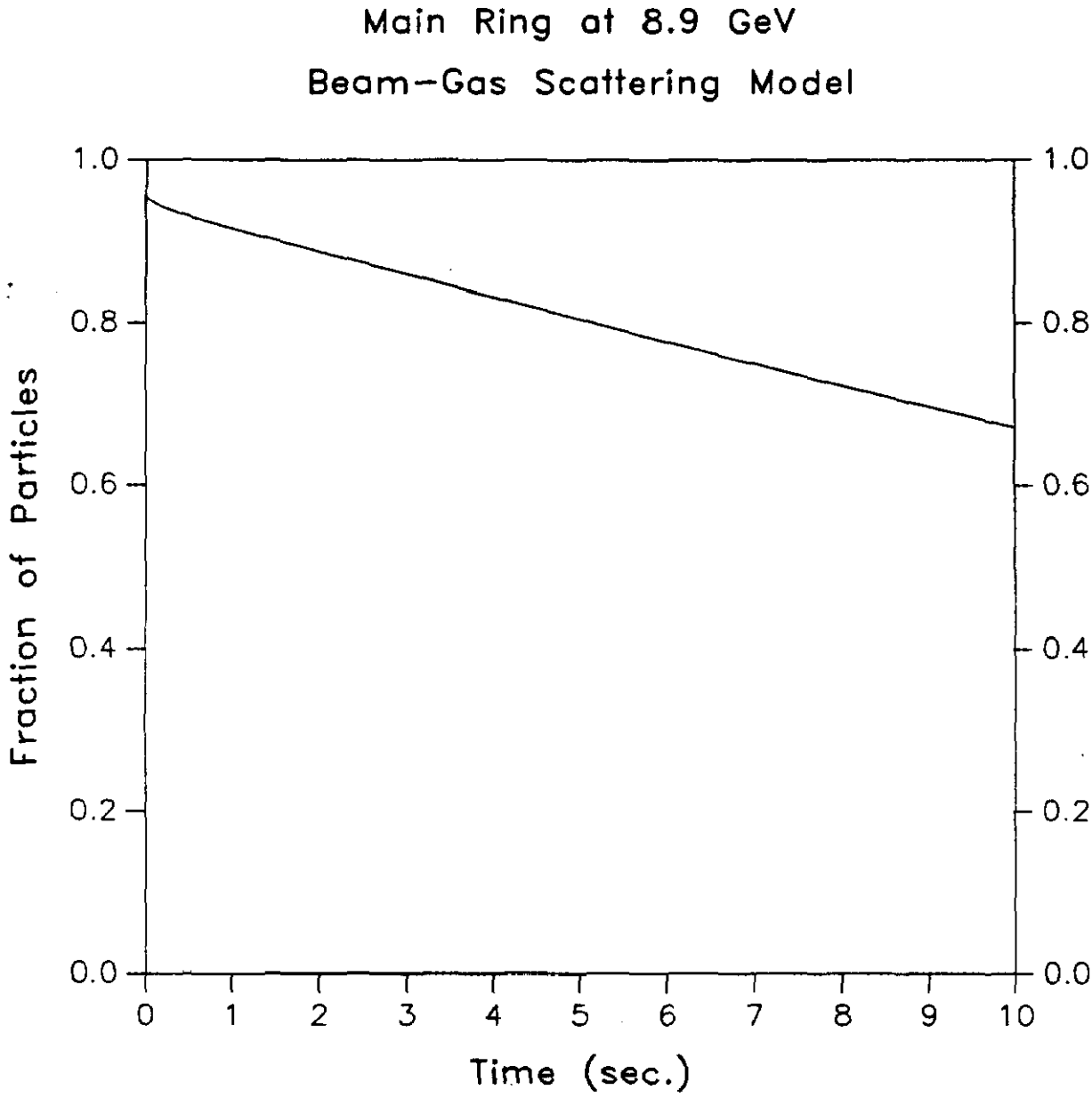

Figure 5. Expected beam intensity plot using Main Ring parameters at 8.9 GeV beam energy.

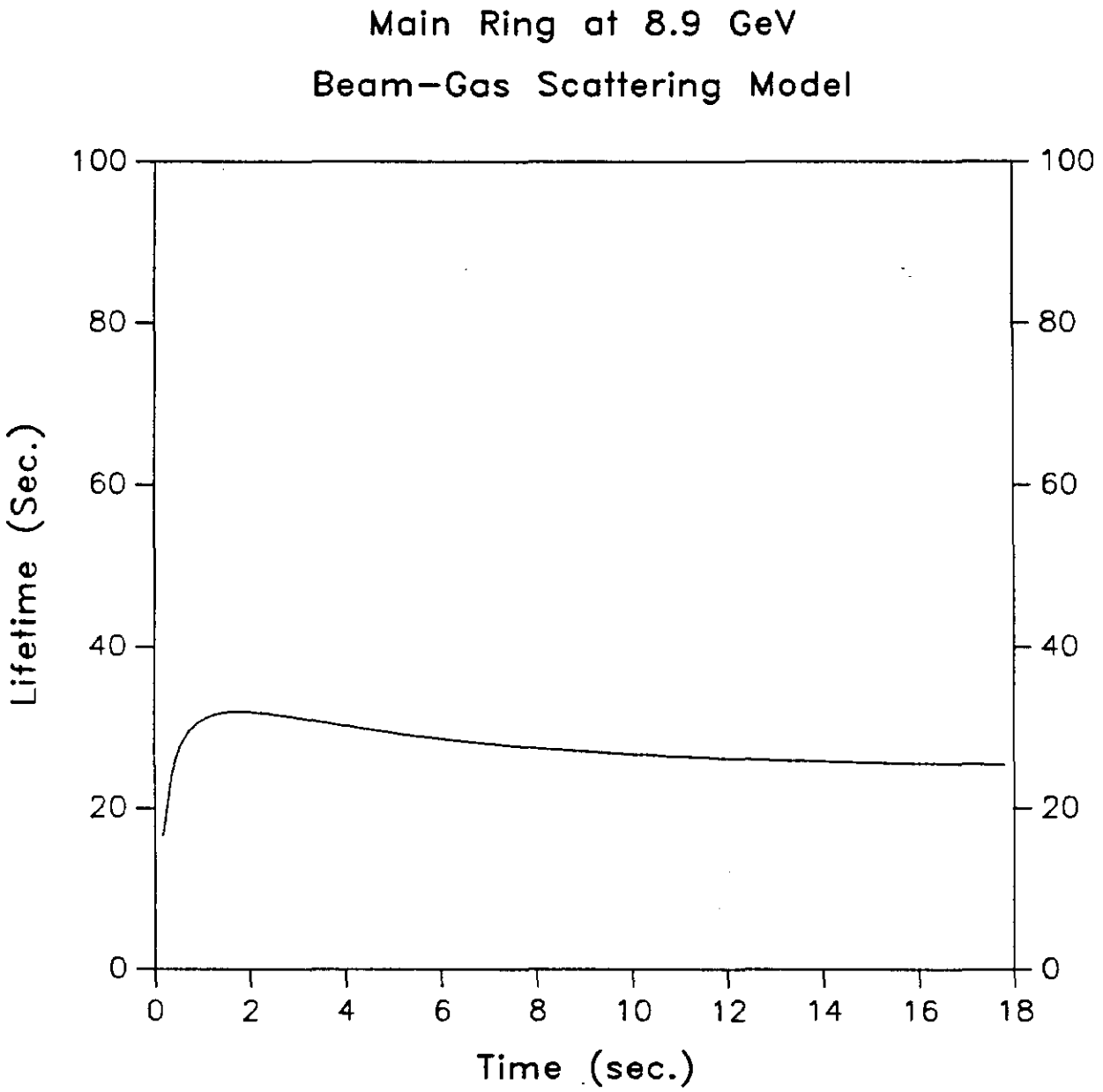

Figure 6. Expected beam lifetime plot using Main Ring parameters at 8.9 GeV beam energy.

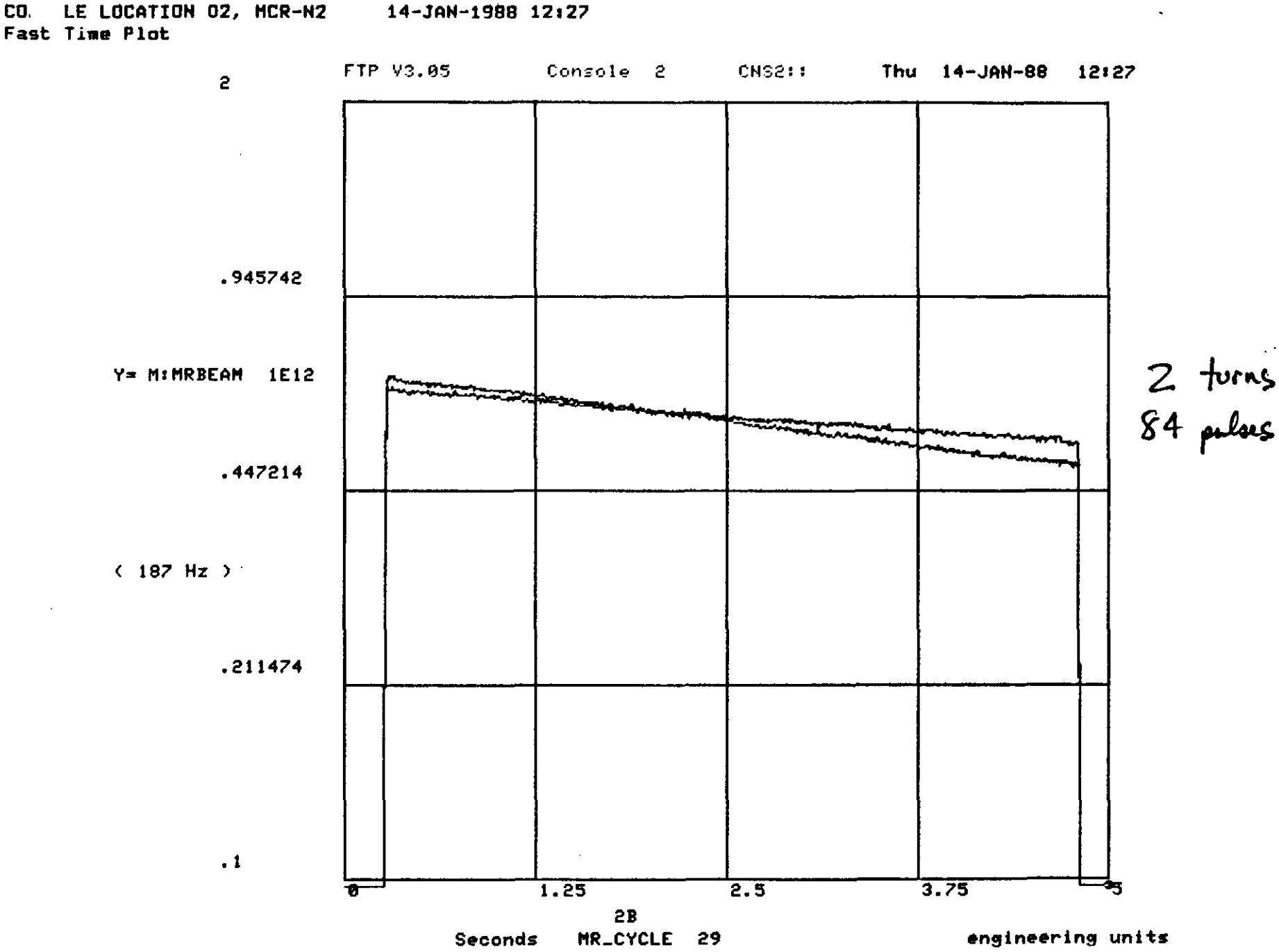

Figure 7. Data taken January 14, 1988 showing 8.9 GeV beam intensity vs. time. Note that the vertical axis is a log scale, more easily allowing for the computation of beam lifetimes.

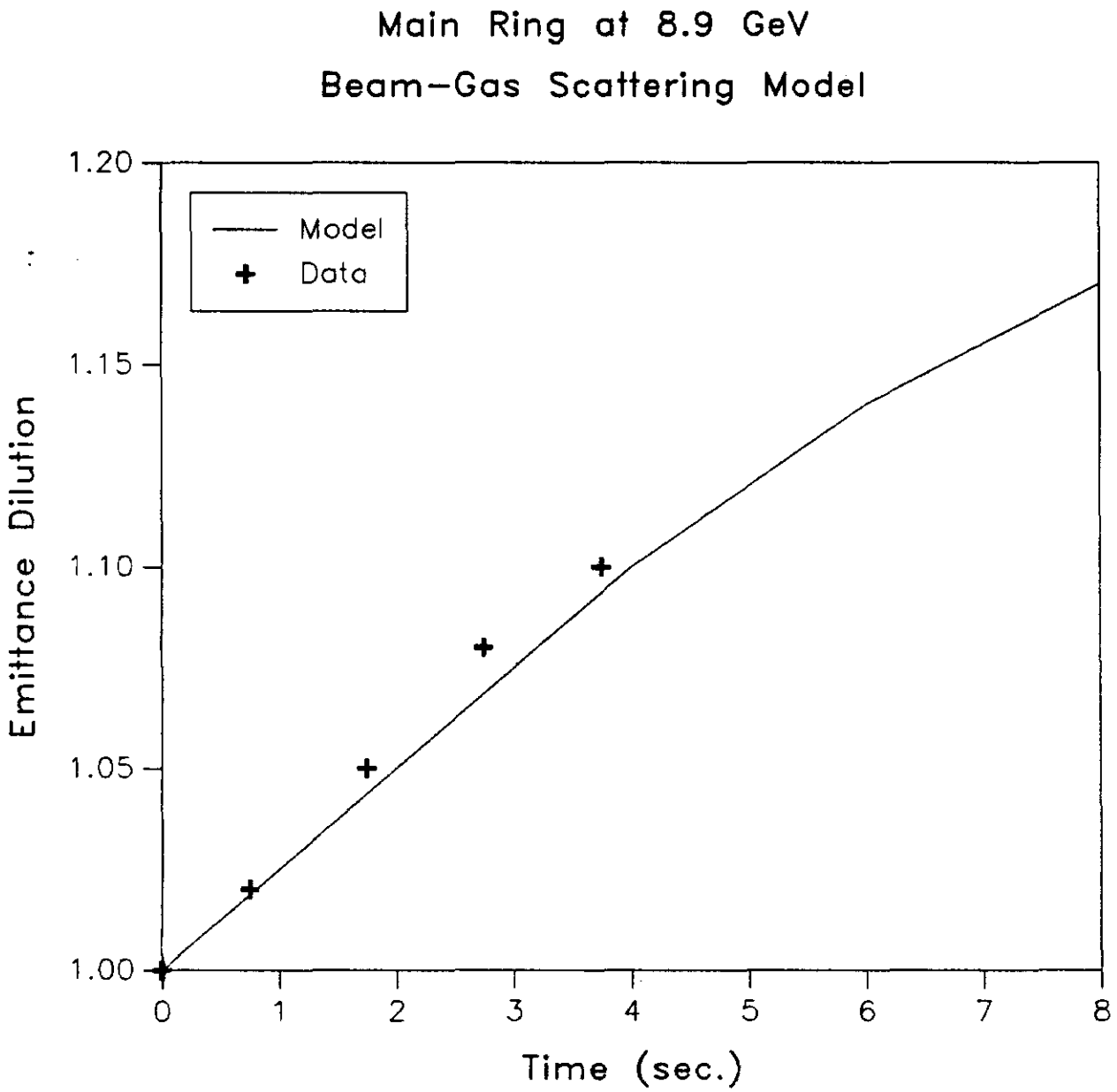

Figure 8. Growth of the vertical emittance in the Main Ring at 8.9 GeV vs. time after injection. The solid line is the prediction from beam-gas scattering; the crosses are data taken January 15, 1988.

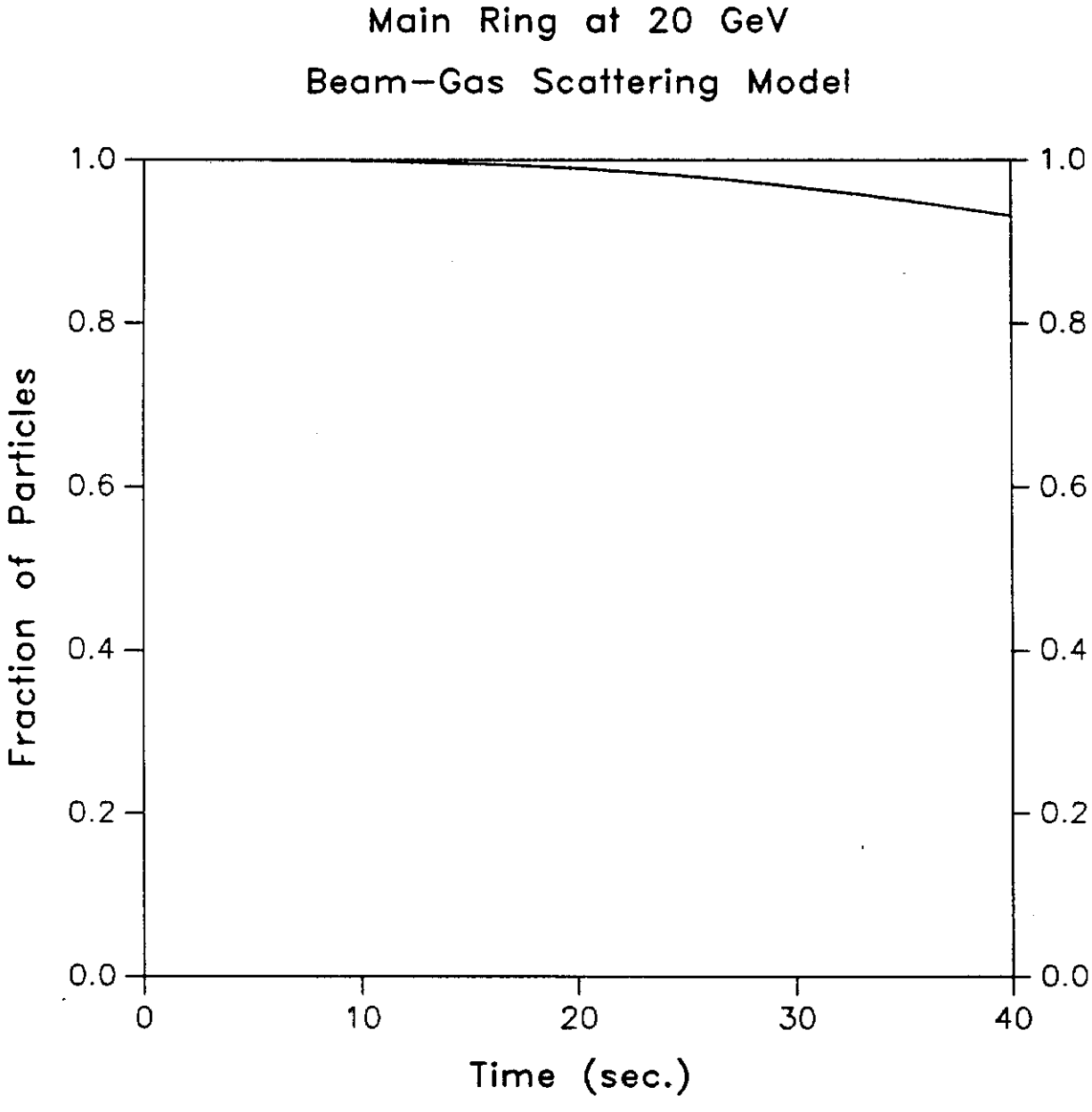

Figure 9. Expected beam intensity plot using Main Ring parameters at 20 GeV beam energy.

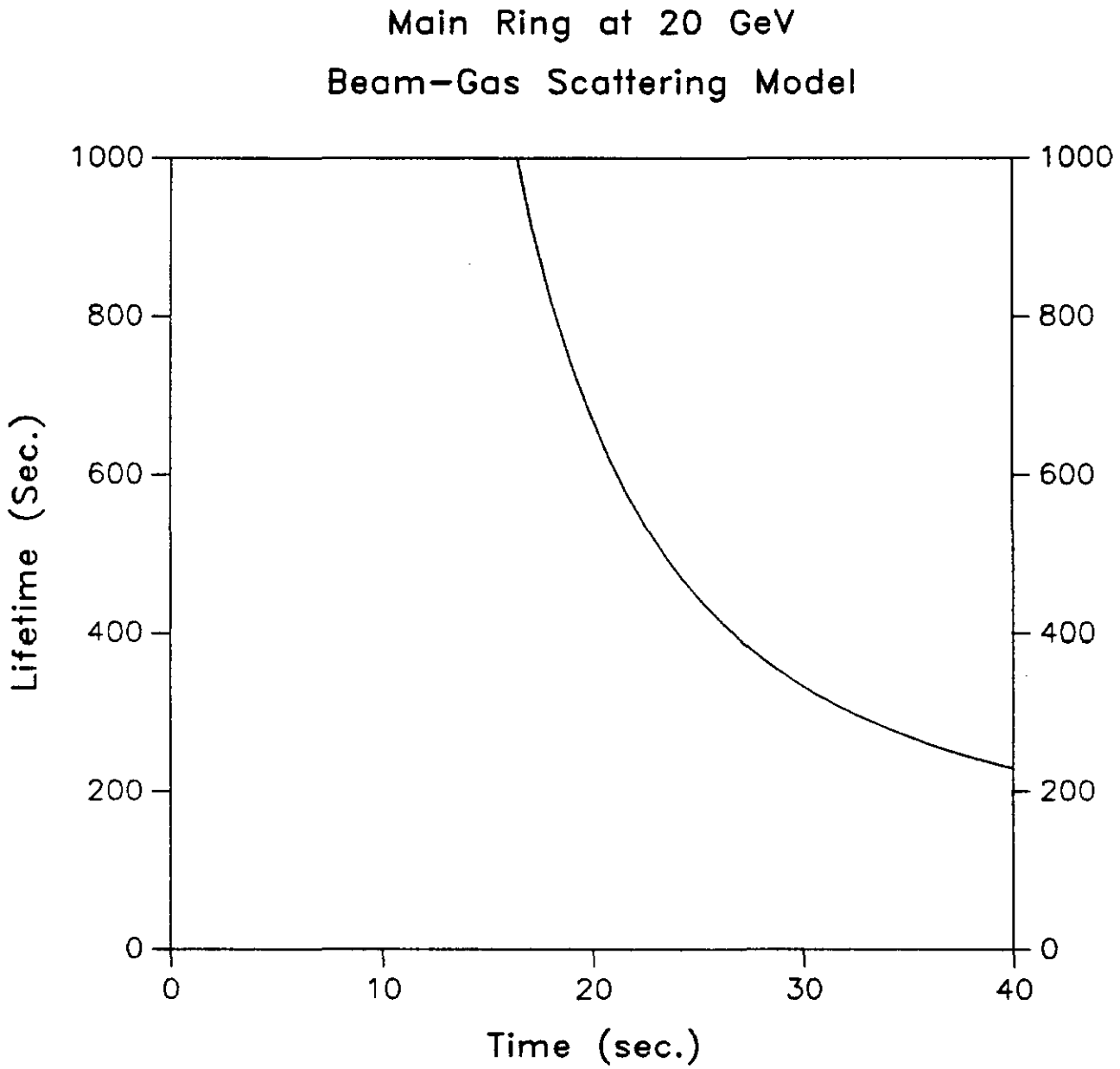

Figure 10. Expected beam lifetime plot using Main Ring parameters at 20 GeV beam energy.

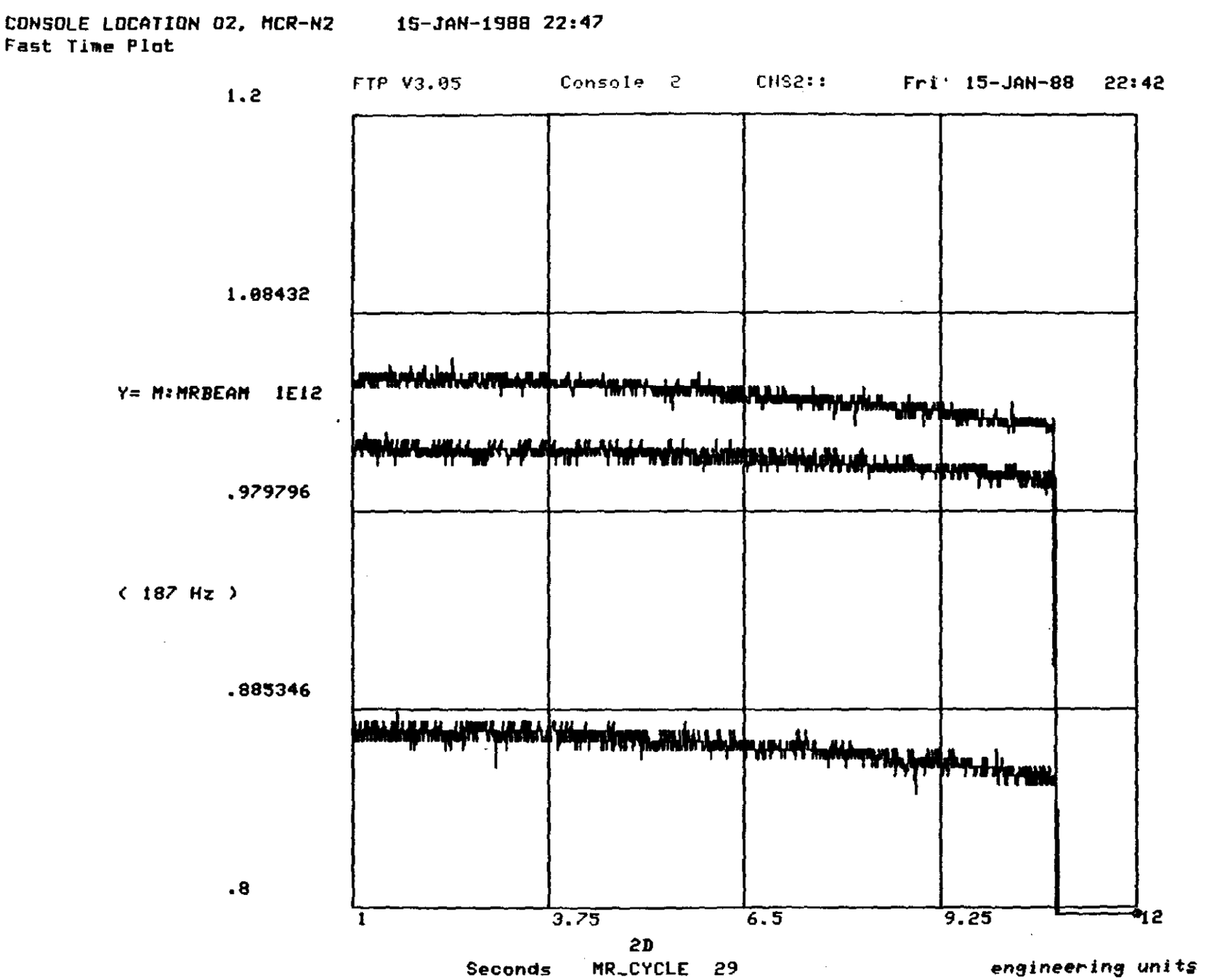

Figure 11. Data taken January 15, 1988 showing 20 GeV beam intensity vs. time. The vertical axis is a log scale, more easily allowing for the computation of beam lifetimes. Note that the intensity remains constant for the first 5 - 6 sec. before gradually decreasing.

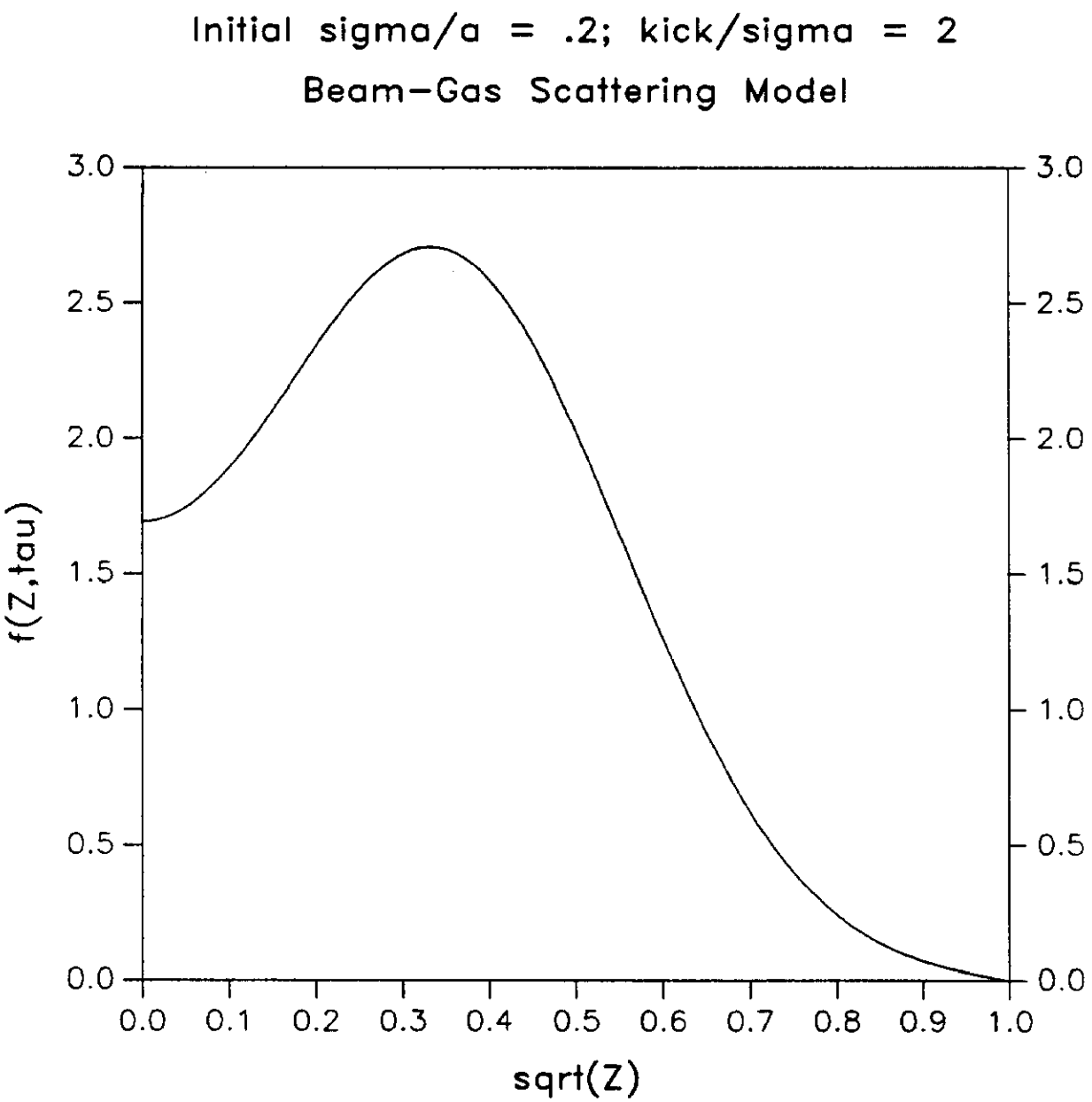

Figure 12. Initial beam distribution used for the analysis of lifetimes of small beams which have been kicked.

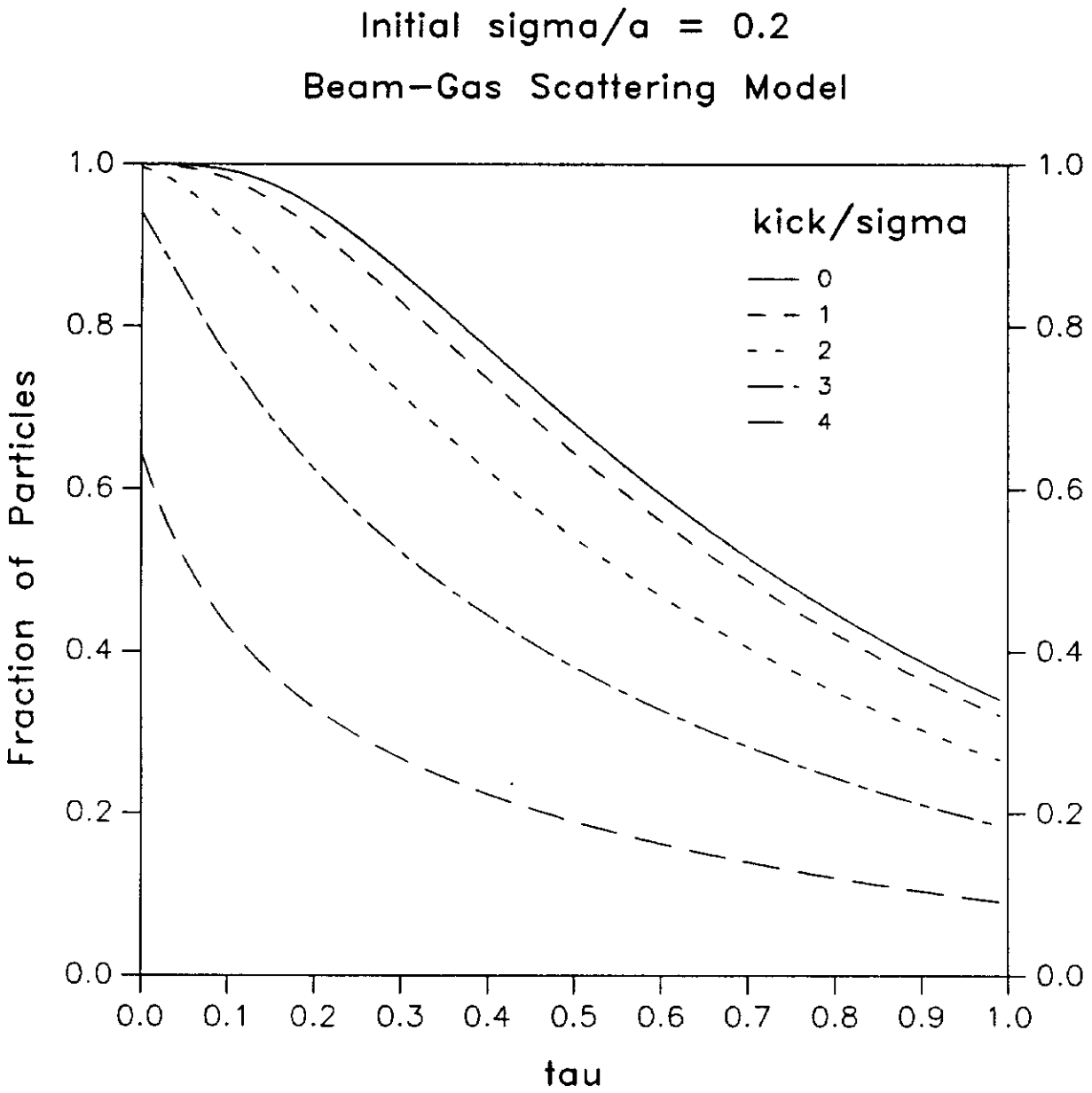

Figure 13. Beam intensity vs. "time" for an initially small beam which has been kicked out to several standard deviations.

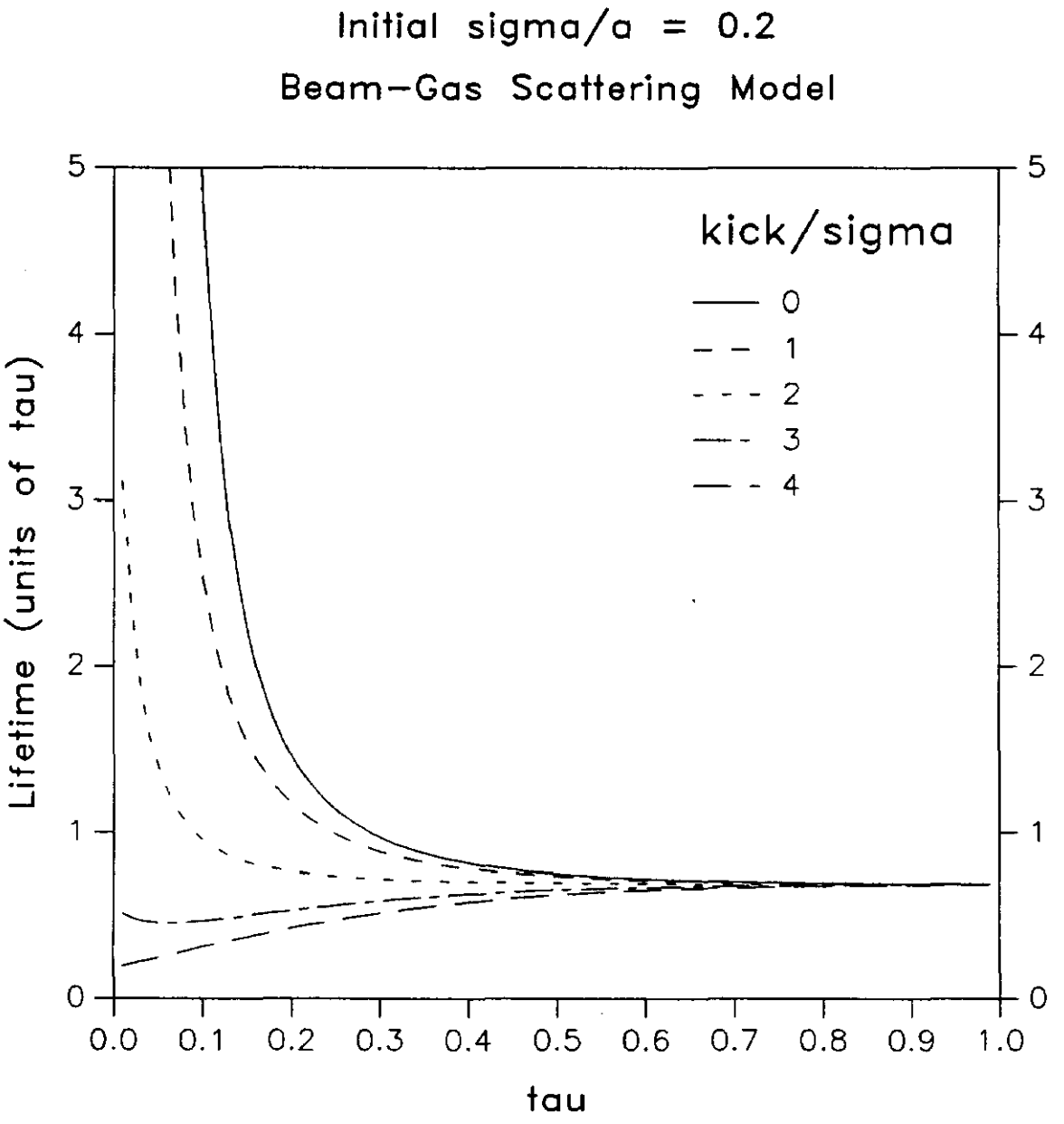

Figure 14. Beam lifetime vs. "time" for the cases presented in Figure 13.

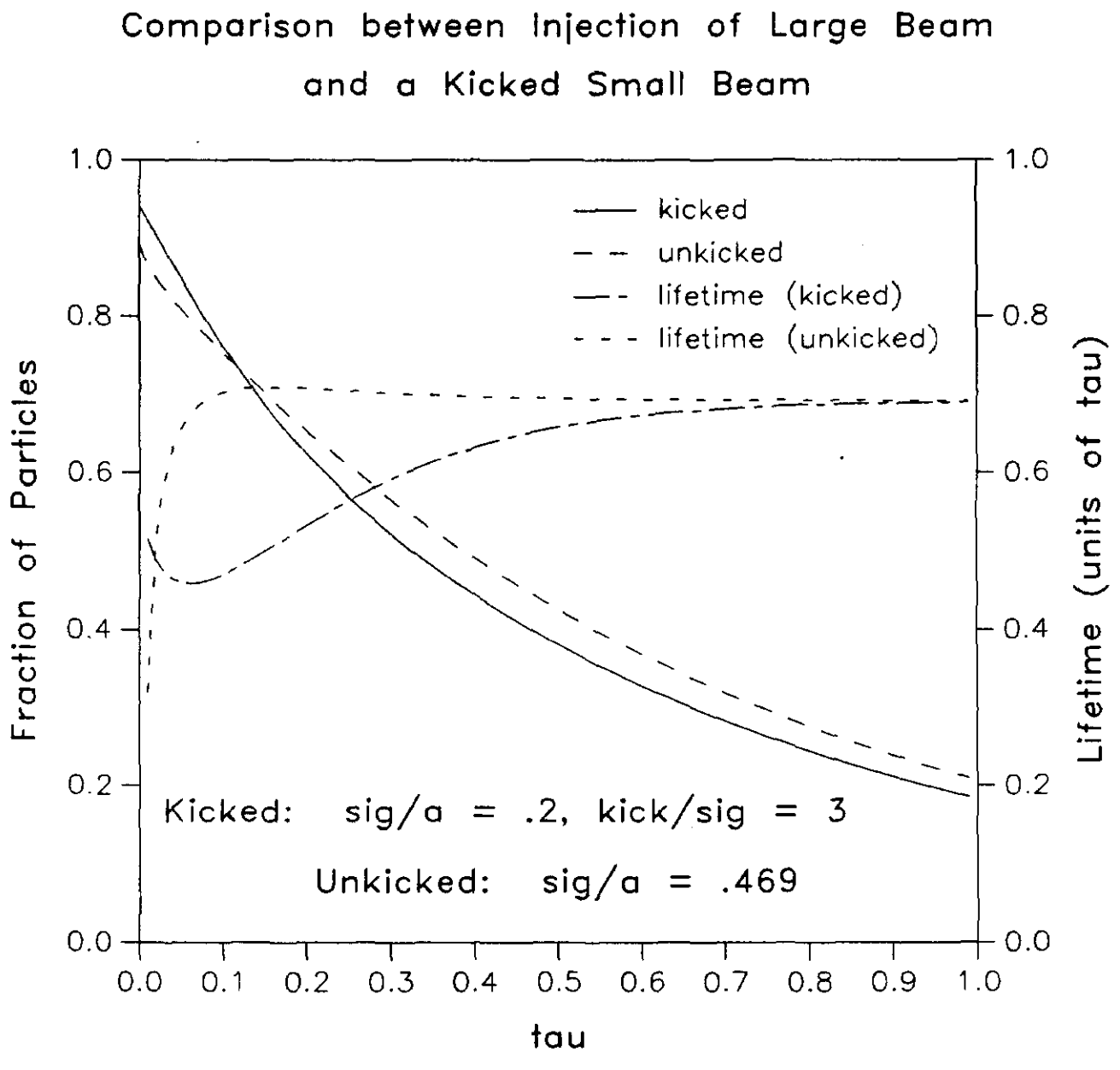

Figure 15. Comparison of beam intensities and lifetimes vs. "time" for the two cases a) injection of a large beam, and b) an initially small beam which has been kicked.

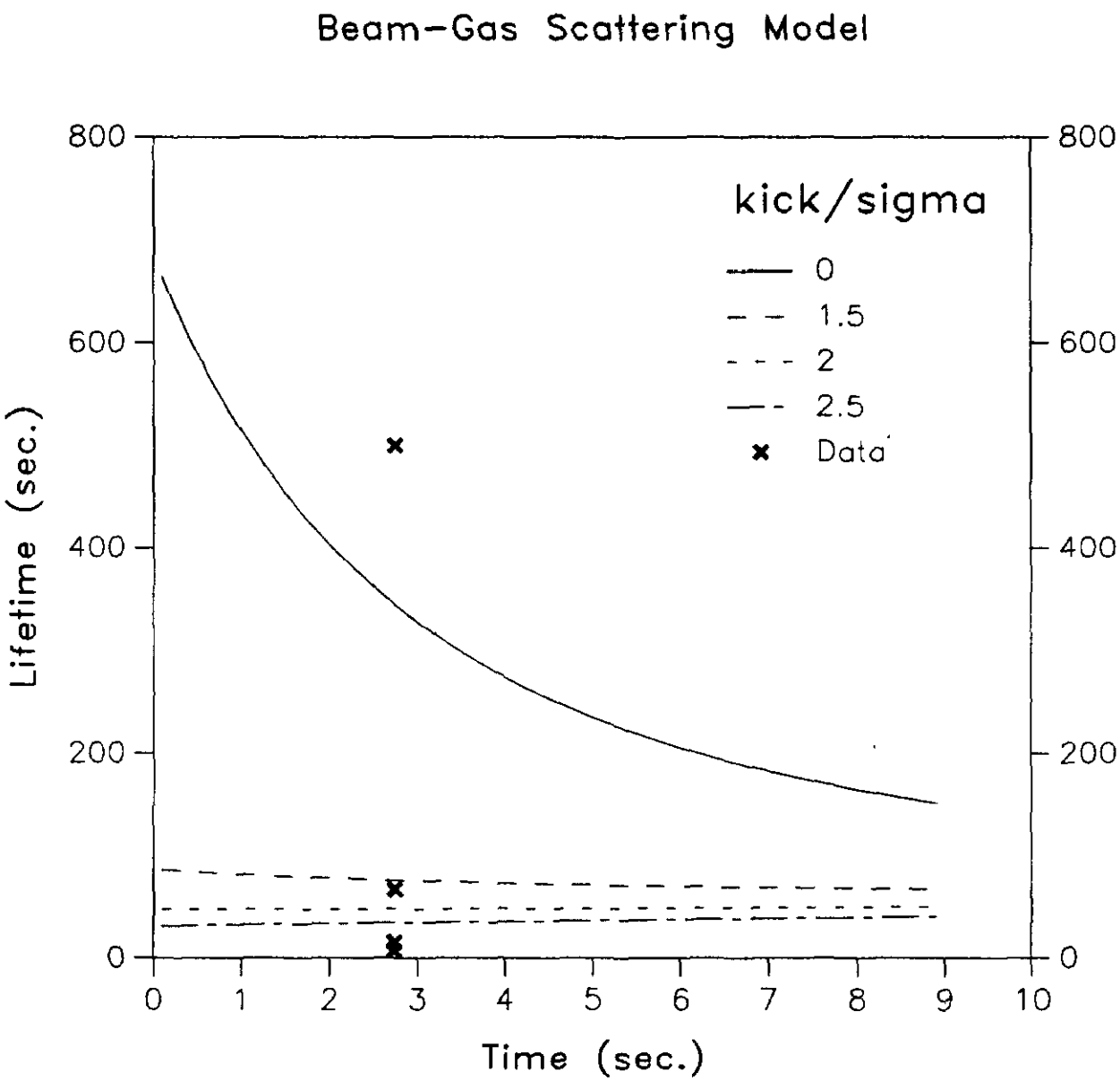

Figure 16. Lifetime vs. time for Main Ring 20 GeV parameters. The curves represent the results of the beam-gas scattering model. The crosses are data taken November 23, 1987.

CONSOLE LOCATION 02, MCR-N2 8-FEB-1988 04:31
Fast Time Plot

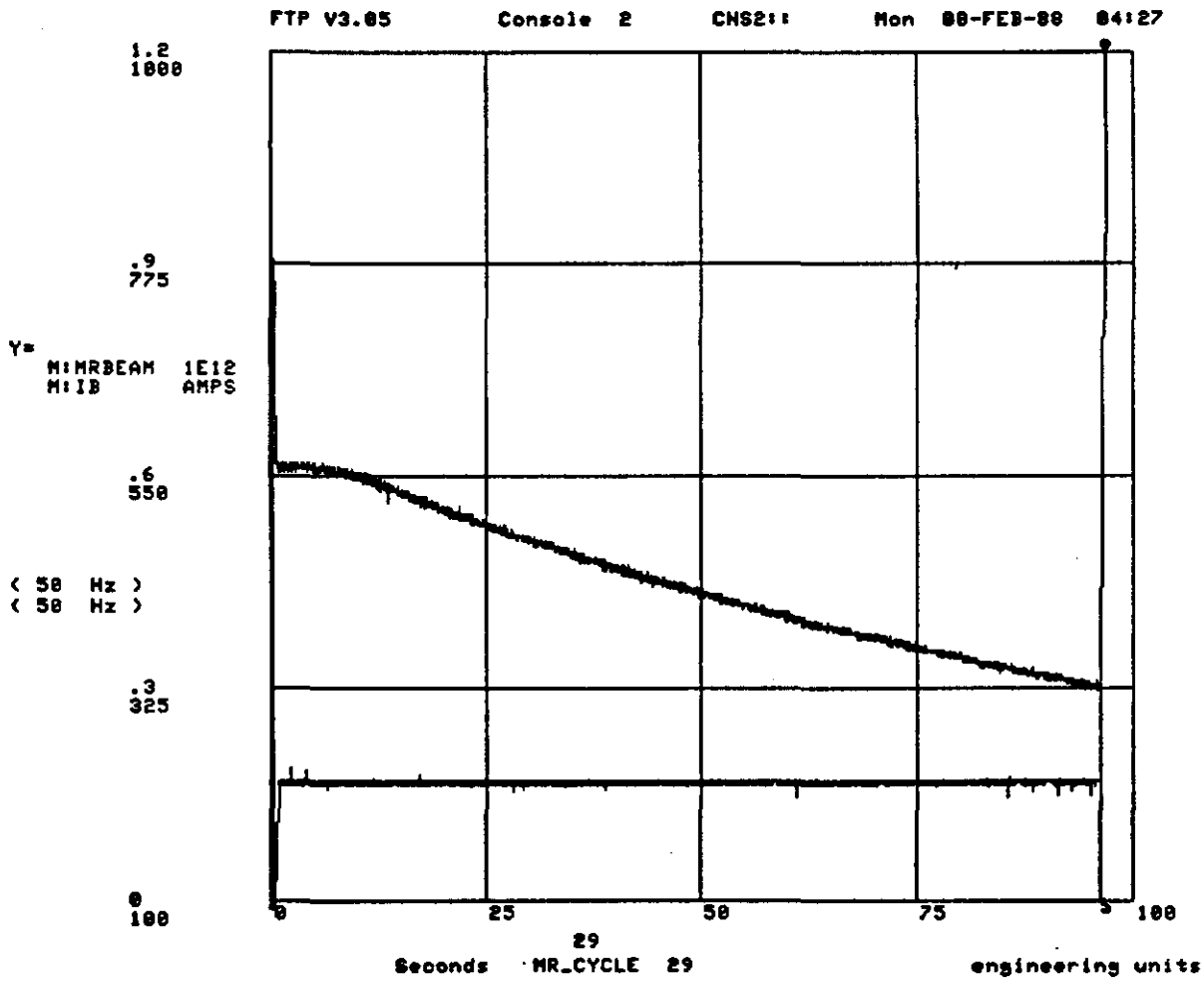

Figure 17. Beam intensity vs. time as observed during a two minute 20 GeV "store" in the Main Ring on February 8, 1988. The second solid curve is the beam current in the Main Ring bend magnets, indicating a store condition.